Generalized Small-Signal Modelling of Dual Active Bridge DC/DC Converter

Osama M. Hebala[1,2,*], Ahmed A. Aboushady[3], Khaled H. Ahmed[4], Sam Burgess[1], Radhakrishna Prabhu[1]

[1]*School of Engineering, Robert Gordon University,* Aberdeen, UK
[2]*Arab Academy for Science, Technology and Maritime Transport (AASTMT),* Alexandria, Egypt
[3]*School of Engineering and Built Environment, Glasgow Caledonian University,* Glasgow, UK
[4]*Department of Electronic & Electrical Engineering, Faculty of Engineering, University of Strathclyde,* Glasgow, UK

[*]Corresponding author: o.m.a.m.hebala@rgu.ac.uk

***Abstract* — this paper presents a novel generalised approach of the small-signal modelling of dual active bridge (DAB) DC/DC converter. The adopted analysis is based on a per-unit fundamental frequency representation of the DAB. The outcome of the proposed modelling approach is a small signal, linearised, state-space DAB model; which is considered as a main building block for future control applications. The developed small signal DAB model includes all possible degrees of freedom affecting the performance of the DAB; this includes the voltage conversion ratio to allow the study of all DAB operation modes (i.e.: unity-gain and buck/boost modes.). Furthermore, since triple phase shift control (TPS) is used in this development work, the proposed model incorporates phase shift in addition to duty ratios. This feature allows for bridge voltage regulation, which is essential for efficient DAB operation in the case of buck/boost operation. Another key achievement is that the proposed small signal modelling methodology can be applied to any bidirectional DC-DC converter regardless of ratings, parameter values and number of ports. Extensive simulation is carried out to verify the proposed analysis.**

Keywords—Dual active bridge (DAB), Triple phase shift (TPS).

I. INTRODUCTION

The dual active bridge (DAB) converter has attracted research among several bidirectional DC/DC converters [1]. This is due to features such as: high power density, high power handing capability, zero voltage switching (ZVS) characteristics, galvanic isolation in transformer based versions and the possibility of cascaded or modular configuration to enable higher power/higher voltage designs [2-5]. This is why investigative studies have been ongoing to analyse, control and improve the overall performance of the DAB converter [2-7]. Currently, there are challenges regarding DAB control. It has many nonlinear properties and the need to achieve multiple objectives – such as regulating power transfer and minimizing current stresses – is vital without compromising the level of control complexity and real time implementation [6,7]. This has resulted in the requirement to develop an accurate and simple small signal DAB model to facilitate controller design.

In the main there are three different small signal, DAB convertor, modelling techniques reported in the literature. These are divided into: simplified averaged model, continuous-time model and discrete-time model [8]. The simplified averaged model is obtained from the input and output average currents as a function of the transformer ratio [9, 10]; where perturbation and linearization techniques are utilized to develop the small signal model [11]. Another variation of the average model approach presented in the literature incorporates conduction and transformer power losses [12].

In [13] a continuous-time averaged model is developed for the DAB converter, where the state variables are defined as DC and first order terms of capacitor voltage and transformer current. While in [14] the small-signal transfer functions are derived by employing state-space averaged over one half cycle. An accurate small-signal, discrete time, model developed for an automotive DAB converter is presented in [15]; however it does come with a high mathematical computation burden. Discrete-time modelling is also discussed in [16, 17].

Reviewing the aforementioned literature shows that an accurate, yet simple, small signal model taking into consideration the converter voltage conversion ratio, along with all possible inputs and outputs, is overlooked. The proposed modelling technique in this paper is: per-unit, simple and satisfies the need for incorporating all possible system inputs/outputs. It can be considered as a general, yet efficient, way to study power electronic systems given the following reasons:

- The proposed small signal model includes voltage conversion ratio *K,* where $K=V_{dc2}/V_{dc1}$; which allows for studying normal DAB operation (i.e.: unity gain/buck/boost.).
- The proposed small signal model includes the duty ratios (D_1, D_2) allowing for variable duty ratio of bridge voltages; which is essential for efficient DAB (buck/boost) operation.

- The proposed modelling methodology is not system dependent and can be applied to any bidirectional DC-DC converter regardless of ratings, parameter values and number of ports. Therefore, it can be applied to a two port DC-DC converter, such as DAB [6,7,18], and a three port DC-DC converter, such as triple active bridge, TAB, [19, 20].
- The model simplicity facilitates controller design without compromising accuracy.

In this paper the proposed modelling approach is presented and applied on a DAB converter as depicted in Fig.1(a). In this approach the converter is represented by its fundamental, frequency-based, DAB diagram as shown in Fig.1(b). The entire analysis used in this paper is based on a 'transformer-less' DAB: meaning the DAB is based on an AC inductor which is fundamentally the equivalent model of a transformer's leakage inductance. Furthermore, the parasitic resistance of the inductor R_{ac} is also included in the analysis.

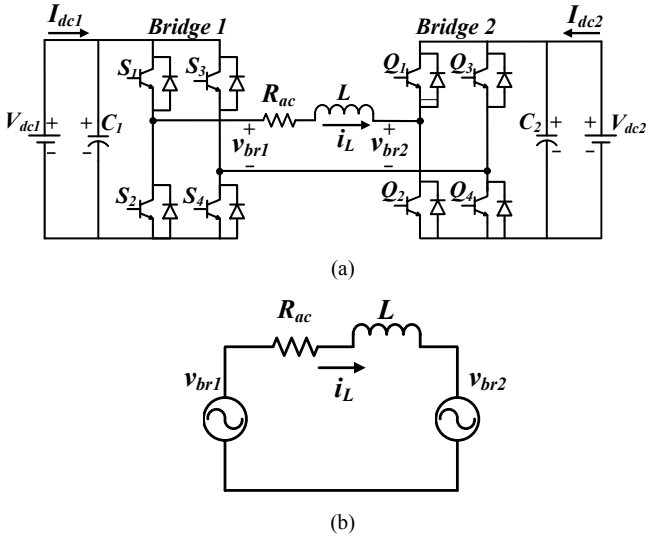

Fig. 1. DAB circuit diagram: (a) Square-wave based DAB, (b) Fundamental-frequency based DAB equivalent circuit.

The paper comprises 7 sections. Section 2 covers the fundamental frequency component of the DAB under TPS control accompanied by the related steady state analytical model. Section 3 presents the proposed small signal methodology and its application on a DAB converter. Afterwards, detailed simulation results are shown in section 4 to validate the developed small signal model. Finally, in section 5, summary conclusions are presented.

II. PER UNIT STEADY STATE ANALYSIS OF DAB

In this section, per unit steady state analysis of the DAB converter is presented. TPS control [6,18] is used in this paper, where the control parameters (D_1, D_2 and D_3) are obtained using classical phase shifting of gate signals S_1-S_4 and Q_1-Q_4 such that $0 \le D_1 \le 1$, $0 \le D_2 \le 1$ and $-1 \le D_3 \le 1$ The ratios D_1 and D_2 represent the pulse width of the first and second bridge voltage waveform (v_{br1}) respectively. Ratio D_3 is the phase shift between positive going edge of v_{br1} and positive going edge of v_{br2}. The definition of TPS is depicted in Fig. 2, where the typical AC voltage/current waveforms of a DAB under TPS control are shown.

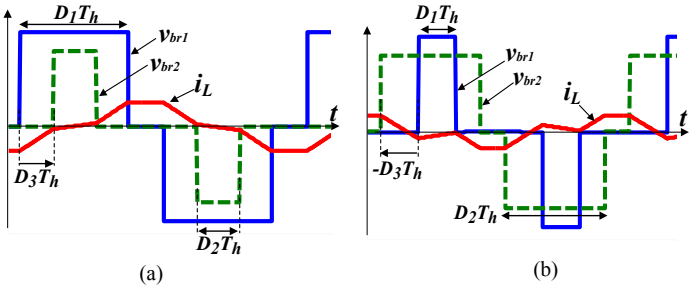

Fig.2. Examples of voltage and currents waveforms for TPS control: (a) Forward (+ve) power flow, and (b) Reverse (-ve) power flow.

The per unit steady state analysis is based on the fundamental frequency approximation [21]; the visual definition of which is presented in Fig. 3 while the equivalent, fundamental frequency-based, analytical representation of the DAB bridge voltages are stated in (1) and (2). The analysis is in per unit, where the base values are selected as: voltage $V_{base}=V_{dc1}$, impedance $Z_{base}=8f_sL$ (f_s is the switching frequency), a time of T_h (half period) and all derived expressions are a function of D_1, D_2, D_3 and K. A factor K is used to describe the voltage conversion ratio (or converter voltage gain), where $K=V_{dc2}/V_{dc1}$: here K=1 represents unity-gain mode and $K\neq1$ represents buck/boost mode.

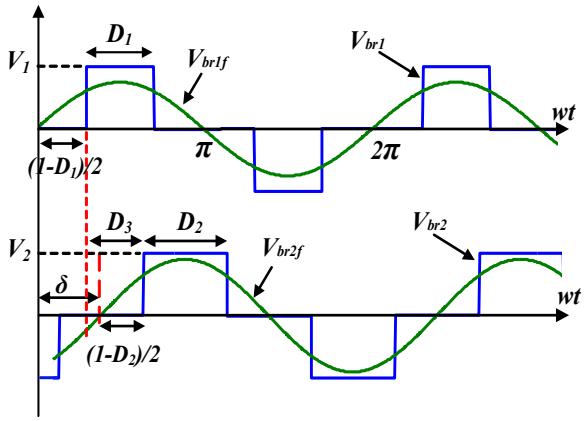

Fig. 3. Definition of phase shift control in fundamental frequency operation

$$v_{br1}(t) = v_{1\,max}\,sin\left(\omega t - (1-D_1)\frac{\pi}{2}\right). \quad (1)$$

$$v_{br2}(t) = v_{2\,max}\,sin\left(\omega t - (1-D_1)\frac{\pi}{2} - \delta\right). \quad (2)$$

Such that,

$$v_{1\,max} = \frac{4}{\pi}sin\left(\frac{D_1\pi}{2}\right), \quad v_{2\,max} = \frac{4K}{\pi}sin\left(\frac{D_2\pi}{2}\right).$$

Where, $$K = \frac{V_{dc2}}{V_{dc1}}$$

and $$\delta = \pi(D_3 + \frac{D_2 - D_1}{2}).$$

III. MODELLING METHODOLGY

The proposed modelling technique is presented in this section. The first step is to express the AC bridge voltages, V_{br1} and V_{br2}, as DC inputs. This is achieved by defining the electrical quantities (i.e: bridge voltage and inductor current.) in equivalent DC components (i.e.: orthogonal DQ components.) such that the DQ component is essentially equivalent to an AC quantity with magnitude and phase angle. The DQ components for DAB variables are defined in (3) and (4).

. (3)

, (4)

$|v_n|$ c , $|v$ |s .

Where,

(1)$\frac{\pi}{}$, (1)– , $\pi(D$ ——) ,

$|v_1|$ – $\left(\frac{D_1\pi}{}\right)$ & $|v_2|$ — $\left(\frac{2}{}\right)$.

A key issue in developing the dynamic model is how to introduce the system dynamics, which is done using (5). Now two steps are required to develop the linear, state space, dynamic DQ model of DAB:

- Separate the bridge voltages, V_{br1} and V_{br2}, along with the inductor current (i_L), into DC components using (3) and (4).
- Add system dynamics using (5).

Applying these steps to (6) yields (7) as follows:

$(v_L)_D = L\frac{}{}i_{L_D}$, $(v_L)_Q = L\frac{}{}i_{L_{DQ}}$. (5)

————. (6)

— (7)

— .

Now, by equating real terms and imaginary terms on both sides of (7) the below outcome is developed:

— –(v). (8)

— –(v). (9)

Further, using the standard state space form outlined by (10), a dynamic DQ-based model of the DAB can be arranged as defined by (11) and (12), where:

- and are states,
- are inputs, and
- and are outputs.

$$\begin{aligned} —[i] &= [A][i] + [B][v]. \\ [i] &= [C][i] + [D][v]. \end{aligned} \quad (10)$$

$$—\begin{bmatrix} i \end{bmatrix} = \begin{bmatrix} —— \\ —— \end{bmatrix}\begin{bmatrix} i^{\,D} \end{bmatrix} + \begin{bmatrix} - & — \\ - & — \end{bmatrix}\begin{bmatrix} \boldsymbol{v} \end{bmatrix}. \quad (11)$$

$$\begin{bmatrix} i^{\,D} \end{bmatrix} = \begin{bmatrix} \end{bmatrix}\begin{bmatrix} i^{\,D} \end{bmatrix} + \begin{bmatrix} \end{bmatrix}\begin{bmatrix} \boldsymbol{v} \end{bmatrix}. \quad (12)$$

The model represented by (10) and (11) includes the system dynamics in addition to the steady state response due to the sinusoidal waveform equivalent of the DQ voltage inputs. However this is a linear state-space DAB model, where it is assumed that the inputs are DQ voltages and the outputs are DQ currents. The main objective is to attain a state space model where the parameters of state space system are defined as follows:

- are states $\bar{X}$,
- are inputs $\bar{U}$, and
- are outputs $\bar{Y}$.

Since the actual inputs are the duty ratios (D_1, D_2) along with the phase shift (D_3), and actual outputs are the power of each bridge (P_{br1}, P_{br2}), along with the RMS current of the AC link ($i_{L_{RMS}}$); therefore actual inputs/outputs need to be mapped to DQ input/outputs, which is where the non-linearity starts to get introduced as shown in (13) and (14).

$$—\begin{bmatrix} i^{\,D} \end{bmatrix} = \begin{bmatrix} —— \\ —— \end{bmatrix}\begin{bmatrix} i^{\,D} \end{bmatrix} \quad \begin{bmatrix} - & — \\ - & — \end{bmatrix} \begin{matrix} - \; n\left(\frac{1}{}\right)\cos(-(1 \quad)) \\ - \; n\left(\frac{1}{}\right)\mathrm{s}\ (-(1 \quad)) \\ - \; n\left(\frac{2}{}\right)\cos(-(1 \quad) \quad) \\ \lfloor - \; n\left(\frac{2}{}\right)\mathrm{s}\ (-(1 \quad) \quad)\rfloor \end{matrix} \quad (13)$$

$$\begin{bmatrix} \quad \end{bmatrix} = \begin{matrix} \left(- \; sin\left(——\right)\cos\left(-(1 \quad)\right) + - \; sin\left(——\right)\mathrm{si}\ \left(-(1 \quad)\right)\right) \\ \left(— \; sin\left(——\right)\cos\left(-(1 \quad) - \quad\right) + — \; sin\left(——\right)\mathrm{si}\ \left(-(1 \quad) \quad\right)\right) \\ \lfloor \qquad\qquad \left(\frac{}{\sqrt{2}}\right) + \left(\frac{Q}{\sqrt{2}}\right) \qquad\qquad \rfloor \end{matrix} \quad (14)$$

Equations (13) and (14) represent the non-linear state-space DAB model where the DQ input/outputs are replaced by actual inputs/outputs.

The next step is to linearize the state-space model in (13) and (14) using a small-signal modelling technique around a steady state equilibrium point using Taylor series. The net outcome of this is the small-signal linearized state-space model outlined by (15).

$$\begin{aligned} — [\Delta x] &= [A]\,[\Delta x] + [B][\Delta u]. \\ [\Delta y] &= [C][\Delta x] + [D][\Delta u]. \end{aligned} \tag{15}$$

Where,

$$— |_{(\quad)}, \quad — |_{(\quad)},$$

$$— |_{(\quad)}, \quad — |_{(\quad)},$$

$$\overline{\Delta u} = \left[\Delta \quad\right], \overline{\Delta y} = \left[\quad\right].$$

The values of X_o and Y_o are calculated by setting the derivates to zero in the non-linear equations (13) and (14) and solving for the steady state values of the states (i_{L_D} and i_{L_Q}) at given inputs (D).The developed small-signal state space linearised model can be summarised as shown in Fig. 4.

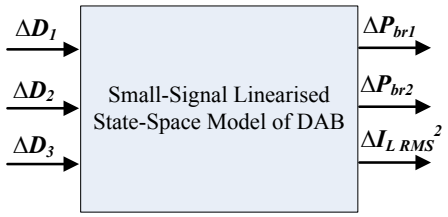

Fig. 4. Inputs & outputs of the small signal linearised model of DAB.

IV. VALIDATION OF THE DEVELOPPED MODEL

Matlab-Simulink has been the main analytical software tool for validating the developed model given by the method illustrated in Fig.5; based on (16) below.

$$\begin{aligned} &x. \\ &u. \\ &y. \end{aligned} \tag{16}$$

Where the following definitions apply:

- $\mathbf{U_o}$ is the input equilibrium operating points selected (D_{1o}, D_{2o}, D_{3o}).
- $\Delta\mathbf{u}$ is defined as perturbations from the equilibrium operating points (ΔD_1, ΔD_2, ΔD_3).
- $\mathbf{X_o}$ is defined as system states evaluated at equilibrium operating points $\mathbf{U_o}$
- $\Delta\mathbf{x}$ is defined as system states evaluated at perturbations from the equilibrium operating points $\Delta\mathbf{u}$
- $\mathbf{Y_o}$ is defined as the system's outputs evaluated at the equilibrium operating conditions $\mathbf{U_o}$ and $\mathbf{X_o}$.
- $\Delta\mathbf{y}$ is defined as the output of the linearised small-signal state space model ($\Delta P_{br1}, \Delta P_{br2}, \Delta {i_{L_{RMS}}}^2$).

Simulations are carried out where perturbations of TPS parameters (D_1, D_2 &D_3) up to ±0.05% around an operating point are applied and the resultant plots are shown in Fig 6 and 7 comparing the outputs from the developed proposed state-space linearised DAB model (Y_{model}) and the detailed DAB circuit (Y_{dab}) in (P_{br1}), (P_{br2}) and ($i_{L_{RMS}}$).

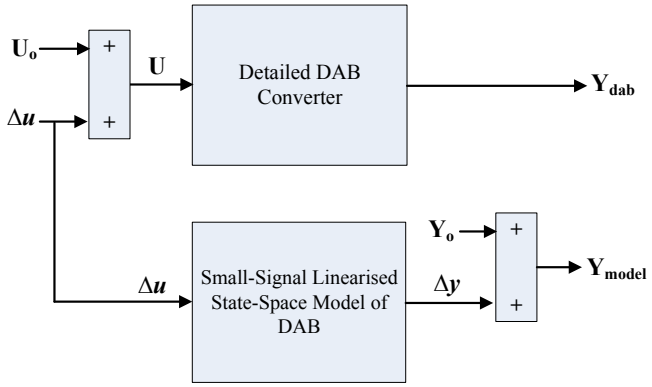

Fig. 5. Validation method of the small-signal state-space DAB model in simulation.

Time domain simulations are carried out, as shown in Fig. 6 and 7, to show how the different state variables behave in the actual non-linear system (detailed switching converter) and how they behave from the proposed small-signal model. The simulation included perturbations with respect to two different test operating points:

- Test point 1 (see Fig.6): U_o=[0.6,0.9,-0.1] resulting in X_o=[0.424,-0.668] and Y_o=[0.121,-0.117, 0.5596^2], at K=0.4.
- Test point 2 (see Fig. 7): U_o=[0.9,0.5, 0.25] resulting in X_o=[0.56,-0.509] and Y_o=[0.082,-0.0811,0.5354^2], at K=0.8.

The simulations were carried out with the DAB parameters described in Table I.

TABLE I
PARAMETERS OF DAB IN SIMULATION

Parameter	value
Bridge 1 DC Voltage V_{dc1}	100V
Bridge 2 DC Voltage V_{dc2}	K*100V
Switching Frequency f_s	2.5kHz
Base Power P_{base}	500W
Interface inductor L	1mH
Parasitic resistance of the inductor R_{ac}	0.05Ω

Fig.6 and 7 show the steady state values of Y_o match the values calculated from the model Y_{model}, in addition where a very small difference is noticed between the state-space linearised DAB model and the detailed DAB circuit such that %error < 2%; i.e.: $Y_{model} \approx Y_{dab}$. This verifies the correctness and reliability of the developed linearised, state-space, small-signal model and the adopted modeling technique.

V. CONCLUSION

This paper has presented and discussed a novel small signal modelling technique applied on a dual active bridge (DAB). The output is a small signal, linearised, state space model of a DAB converter. The key features of this model are: high accuracy, simplicity and consideration of all possible system inputs/outputs. The proposed modelling approach is also generic and can be applied to any bidirectional DC-DC converter regardless of ratings, parameter values and number of ports. The reliability of the proposed modelling technique is confirmed within the simulation results presented.

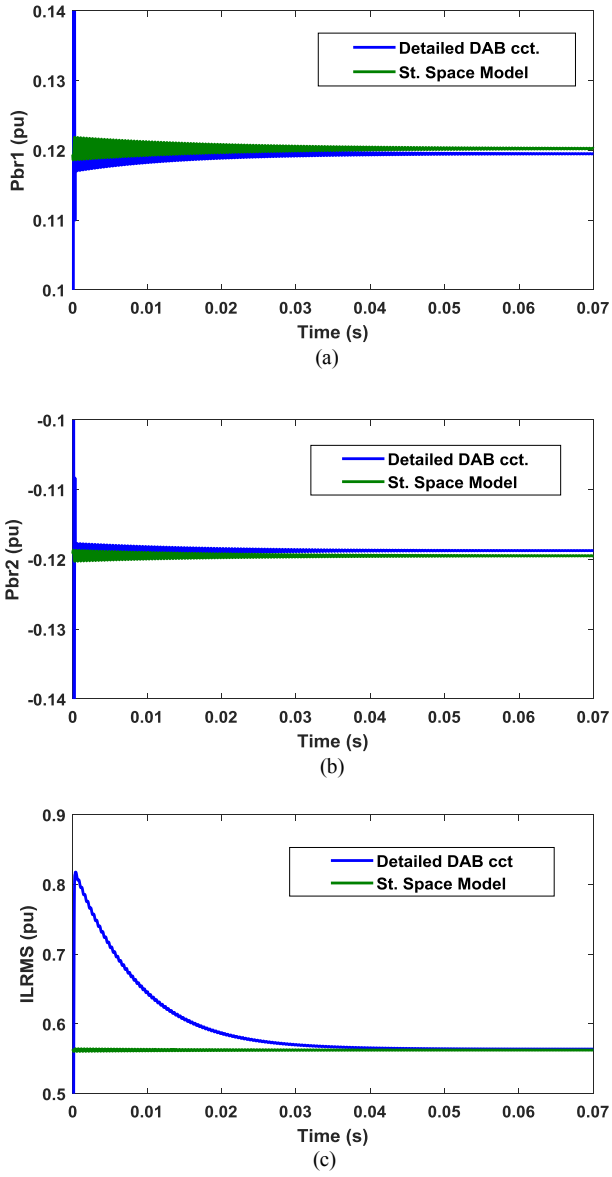

Fig 6. Comparative analysis of outputs from the proposed small-signal state-space DAB model (Y_{model}) and outputs of the detailed DAB circuit (Y_{dab}) at operating point U_o=[0.6,0.9,-0.1] for K=0.4: (a) P_{br1}, (b) P_{br2} and (c) $i_{L\,RMS}$.

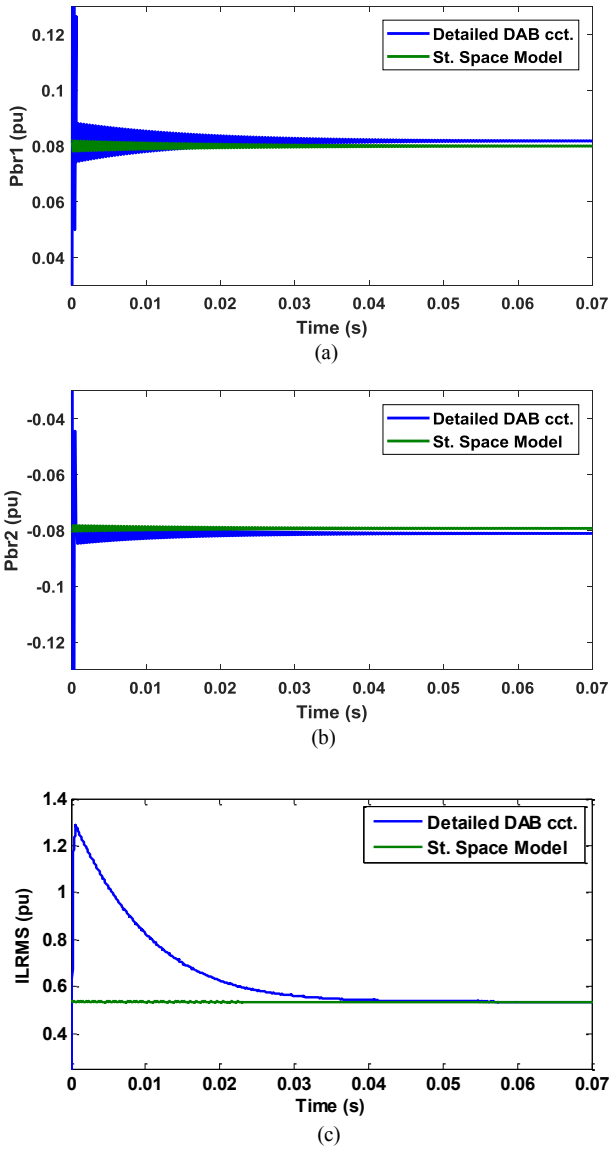

Fig 7. Comparative analysis of outputs from the proposed small-signal state-space DAB model (Y_{model}) and outputs of the detailed DAB circuit (Y_{dab}) at operating point Uo=[0.9,0.5, 0.25] for K=0.8: (a) P_{br1}, (b) P_{br2} and (c) $i_{L\,RMS}$.

REFERENCES

[1] B. Zhao, Q. Song, W. Liu and Y. Sun, "Overview of Dual-Active-Bridge Isolated Bidirectional DC–DC Converter for High-Frequency-Link Power-Conversion System," in IEEE Transactions on Power Electronics, vol. 29, no. 8, pp. 4091-4106, Aug. 2014.

[2] B. Zhao, Q. Song, J. Li, Q. Sun and W. Liu, "Full-Process Operation, Control, and Experiments of Modular High-Frequency-Link DC Transformer Based on Dual Active Bridge for Flexible MVDC Distribution: A Practical Tutorial," in IEEE Transactions on Power Electronics, vol. 32, no. 9, pp. 6751-6766, Sept. 2017.

[3] J. Riedel, D. G. Holmes, B. P. McGrath and C. Teixeira, "Active Suppression of Selected DC Bus Harmonics for Dual Active Bridge DC–DC Converters," in IEEE Transactions on Power Electronics, vol. 32, no. 11, pp. 8857-8867, Nov. 2017.

[4] S. T. Lin, X. Li, C. Sun and Y. Tang, "Fast transient control for power adjustment in a dual-active-bridge converter," in Electronics Letters, vol. 53, no. 16, pp. 1130- 1132, 8 3 2017.
[5] M. Yaqoob, K. H. Loo and Y. M. Lai, "Extension of Soft-Switching Region of Dual-Active-Bridge Converter by a Tunable Resonant Tank," in IEEE Transactions on Power Electronics, vol. 32, no. 12, pp. 9093-9104, Dec. 2017.
[6] O. M. Hebala, A. Aboushady, K. H. Ahmed and I. A. Abdelsalam, "Generic Closed Loop Controller for Power Regulation in Dual Active Bridge DC/DC Converter with Current Stress Minimization," in *IEEE Transactions on Industrial Electronics*.
[7] N. Hou, W. Song and M. Wu, "Minimum-Current-Stress Scheme of Dual Active Bridge DC–DC Converter With Unified Phase-Shift Control," in IEEE Transactions on Power Electronics, vol. 31, no. 12, pp. 8552-8561, Dec. 2016.
[8] F. L. F. Marcelino, H. H. Sathler, T. R. de Oliveira and P. F. Donoso-Garcia, "Modeling and control of a Dual Active Bridge for energy storage in DC microgrid applications," *2017 IEEE 8th International Symposium on Power Electronics for Distributed Generation Systems (PEDG)*, Florianopolis, 2017, pp. 1-8.
[9] A. Rodríguez Alonso, J. Sebastian, D. G. Lamar, M. M. Hernando and A. Vazquez, "An overall study of a Dual Active Bridge for bidirectional DC/DC conversion," *2010 IEEE Energy Conversion Congress and Exposition*, Atlanta, GA, 2010, pp. 1129-1135.
[10] H. K. Krishnamurthy and R. Ayyanar, "Building Block Converter Module for Universal (AC-DC, DC-AC, DC-DC) Fully Modular Power Conversion Architecture," *2007 IEEE Power Electronics Specialists Conference*, Orlando, FL, 2007, pp. 483-489.
[11] Erickson, R. W.; Maksimovic, D. Fundamentals of Power Electronics.2ed. Springer, 2001.
[12] K. Zhang, Z. Shan and J. Jatskevich, "Large- and Small-Signal Average-Value Modeling of Dual-Active-Bridge DC–DC Converter Considering Power Losses," in *IEEE Transactions on Power Electronics*, vol. 32, no. 3, pp. 1964-1974, March 2017.
[13] H. Qin and J. W. Kimball, "Generalized Average Modeling of Dual Active Bridge DC–DC Converter," in *IEEE Transactions on Power Electronics*, vol. 27, no. 4, pp. 2078-2084, April 2012.
[14] G. D. Demetriades and H. Nee, "Dynamic modeling of the Dual-Active Bridge topology for high-power applications," *2008 IEEE Power Electronics Specialists Conference*, Rhodes, 2008, pp. 457-464.
[15] F. Krismer and J. W. Kolar, "Accurate Small-Signal Model for the Digital Control of an Automotive Bidirectional Dual Active Bridge," in *IEEE Transactions on Power Electronics*, vol. 24, no. 12, pp. 2756-2768, Dec. 2009.
[16] Ling Shi, Wanjun Lei, Jun Huang, Zhuoqiang Li, Yao Cui and Yue Wang,"Full discrete-time modeling and stability analysis of the digital controlled dual active bridge converter," 2016 IEEE 8th International Power Electronics and Motion Control Conference (IPEMC-ECCE Asia), Hefei, 2016, pp. 3813-3817.
[17] D. Costinett, R. Zane and D. Maksimovi, "Discrete-time small-signal modeling of a 1 MHz efficiency-optimized dual active bridge converter with varying load," 2012 IEEE 13th Workshop on Control and Modeling for Power Electronics (COMPEL), Kyoto, 2012, pp. 1-7.
[18] J. Huang, Y. Wang, Z. Li and W. Lei, "Unified Triple-Phase-Shift Control to Minimize Current Stress and Achieve Full Soft-Switching of Isolated Bidirectional DC–DC Converter," in IEEE Transactions on Industrial Electronics, vol. 63, no. 7, pp. 4169-4179, July 2016.
[19] O. M. Hebala, A. A. Aboushady and K. H. Ahmed, "Analysis of AC link topologies in non-isolated DC/DC triple active bridge converter for current stress minimization," *2017 IEEE 6th International Conference on Renewable Energy Research and Applications (ICRERA)*, San Diego, CA, 2017, pp. 608-613.
[20] C. Zhao, S. D. Round and J. W. Kolar, "An Isolated Three-Port Bidirectional DC-DC Converter With Decoupled Power Flow Management," in *IEEE Transactions on Power Electronics*, vol. 23, no. 5, pp. 2443-2453, Sept. 2008.
[21] B. Zhao, Q. Song, W. Liu, G. Liu and Y. Zhao, "Universal High-Frequency-Link Characterization and Practical Fundamental-Optimal Strategy for Dual-Active-Bridge DC-DC Converter Under PWM Plus Phase-Shift Control," in *IEEE Transactions on Power Electronics*, vol. 30, no. 12, pp. 6488-6494, Dec. 2015.